Nitrate radical generation via continuous generation of dinitrogen pentoxide in a laminar flow reactor coupled to an oxidation flow reactor

Andrew T. Lambe[1], Ezra C. Wood[2], Jordan E. Krechmer[1], Francesca Majluf[1], Leah R. Williams[1], Philip L. Croteau[1], Manuela Cirtog[3], Anaïs Féron[3], Jean-Eudes Petit[4], Alexandre Albinet[5], Jose L. Jimenez[6], and Zhe Peng[6]

[1]Center for Aerosol and Cloud Chemistry, Aerodyne Research Inc., Billerica, MA, USA
[2]Dept. of Chemistry, Drexel University, Philadelphia, PA, USA
[3]Laboratoire Inter-Universitaire des Systèmes Atmosphériques (LISA), UMR CNRS 7583, Université Paris-Est-Créteil, Université de Paris, Institut Pierre Simon Laplace (IPSL), Créteil, France
[4]Laboratoire des Sciences du Climat et de l'Environnement (CNRS-CEA-UVSQ), CEA Orme des Merisiers, Gif-sur-Yvette, France
[5]Institut National de l'Environnement Industriel et des Risques (Ineris), Verneuil-en-Halatte, France
[6]Dept. of Chemistry and Cooperative Institute for Research in Environmental Sciences (CIRES), University of Colorado, Boulder, CO, USA

Correspondence: Andrew T. Lambe (lambe@aerodyne.com), Zhe Peng (zhe.peng@colorado.edu)

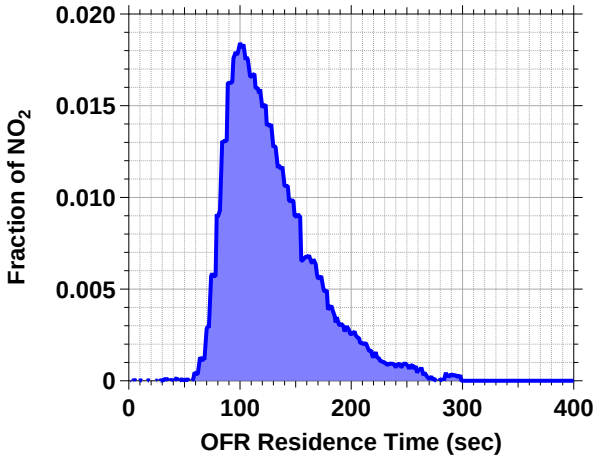

Figure S1. Residence time distribution of 10 s pulsed inputs of NO_2 injected into the Potential Aerosol Mass OFR obtained with lights off and 6.5 L min^{-1} flow through the reactor.

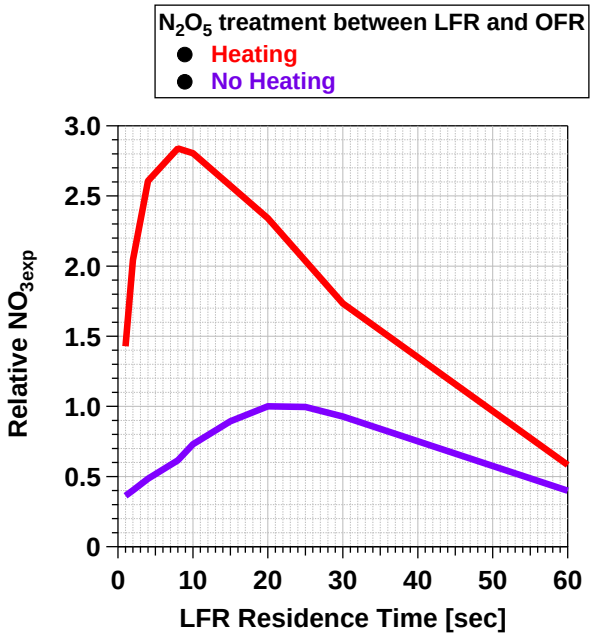

Figure S2. Model simulations of the relative NO_{3exp} achieved in the OFR following injection of 300 ppm O_3 and NO_2 into the LFR as a function of τ_{LFR} ranging from 1 to 60 s. Purple and red lines represent modeling cases corresponding to 0% ("no heating") and 100% ("heating") thermal dissociation of N_2O_5 between the LFR and OFR.

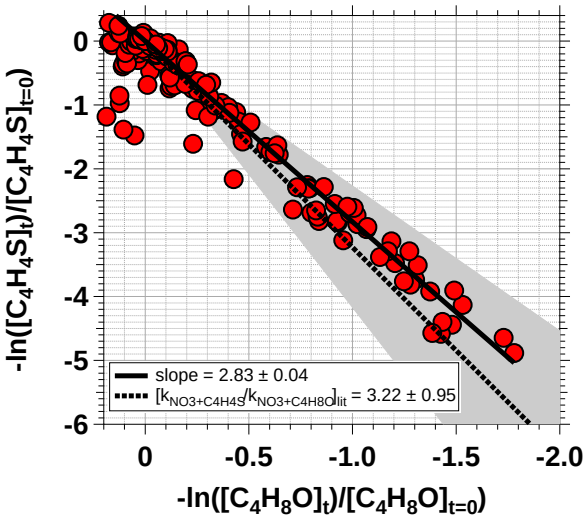

Figure S3. Relative rate constant obtained from PTR-MS measurements of butanal (C_4H_8O) and thiophene (C_4H_4S) tracers used in OFR-iN_2O_5 characterization studies. Literature relative rate constant obtained from kinetic data published by Atkinson (1991) and D'Anna et al. (2001).

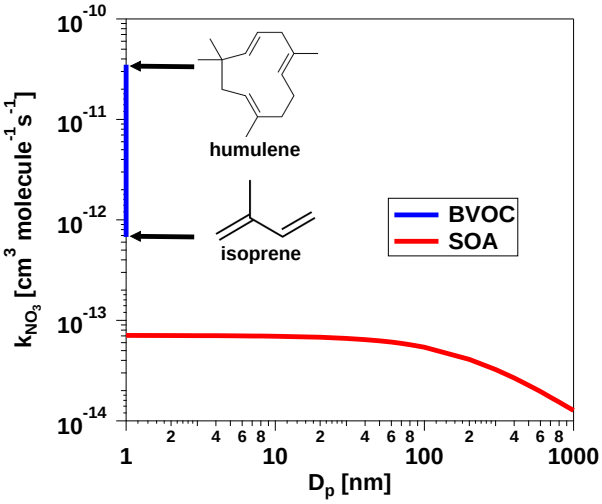

Figure S4. Effective rate constant between NO_3 and SOA particles (k_{NO_3}) calculated using Eq. 6 assuming ρ_p = 1.4 g cm^{-3}, M_{SOA} = 250 g mol^{-1} and γ = 0.1.

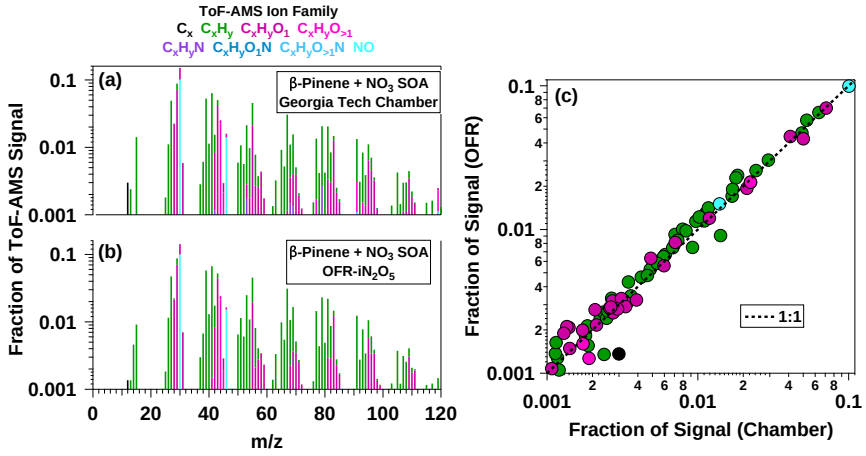

Figure S5. Logarithmically scaled AMS spectra of SOA generated from NO_3 oxidation of β-pinene in the (a) Georgia Tech environmental chamber (Boyd et al., 2015) and (b) OFR. Scatter plot in (c) shows spectra generated in the OFR and chamber plotted against each other.

Table S1. VOC tracers used in OFR-iN_2O_5 characterization studies. Bimolecular rate coefficients for reaction with NO_3 and O_3 are given in units of cm^3 $molecule^{-1}$ s^{-1}.

Compound	Formula	Structure	k_{NO_3}	k_{O_3}	References
Acetonitrile	C_2H_3N	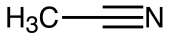	$<3.01\times10^{-19}$	N/A	1
Toluene	C_7H_8	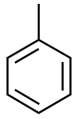	6.79×10^{-17}	3.90×10^{-22}	2,3
o-Xylene	C_8H_{10}	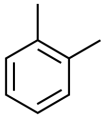	3.77×10^{-16}	1.72×10^{-21}	2,3
p-Cymene	$C_{10}H_{14}$	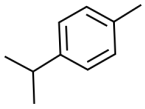	1.00×10^{-15}	$<5.00\times10^{-20}$	2,4
1,2,4-Trimethylbenzene	C_9H_{12}	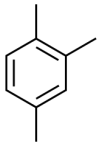	1.81×10^{-15}	$<1.3\times10^{-21}$	2
Butanol	$C_4H_{10}O$	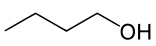	$<2.71\times10^{-15}$	N/A	5
Benzaldehyde	C_7H_6O	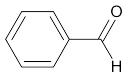	4.3×10^{-15}	$<2.00\times10^{-19}$	2,6
Butanal	C_4H_8O	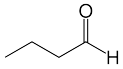	1.22×10^{-14}	N/A	7
Thiophene	C_4H_4S	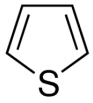	3.94×10^{-14}	5.99×10^{-20}	2,8
2,3-Dihydrobenzofuran	C_8H_8O	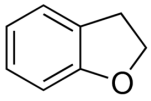	1.15×10^{-13}	$<1.00\times10^{-19}$	2,9
Naphthalene-d8	$C_{10}D_8$	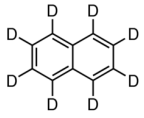	$4.76\times10^{-28}\times[NO_2]$	N/A	2

[1]Cantrell et al. (1987); [2]Atkinson (1991); [3]Toby et al. (1985); [4]Atkinson et al. (1990); [5]Chew et al. (1998); [6]Bernard et al. (2013); [7]D'Anna et al. (2001); [8]Atkinson et al. (1983); [9]Atkinson et al. (1992)

Table S2. KinSim mechanism used to model NO_3 and N_2O_5 formation and destruction in the LFR and OFR. Kinetic data is adapted from mechanism published in Palm et al. (2017) and references therein.

Reactant 1	Reactant 2	Product 1	Product 2	Product 3	A_∞	E_∞	n_∞	A_0	E_0	n_0
NO	O_3	NO_2	O_2		3E-12	1500	0	0	0	0
NO_2	O_3	NO_3	O_2		1.2E-13	2450	0	0	0	0
NO_3	NO_3	NO_2	NO_2	O_2	8.5E-13	2450	0	0	0	0
N_2O_5	H_2O	HNO_3	HNO_3		1E-22	0	0	0	0	0
NO_2	NO_3	N_2O_5			1.9E-12	0	-0.2	3.6E-30	0	4.1
N_2O_5		NO_2	NO_3		9.7E+14	11080	-0.1	0.0013	11000	3.5
NO	NO_3	NO_2	NO_2		1.8E-11	-110	0	0	0	0
NO_2	NO_3	NO	NO_2	O_2	4.5E-14	1260	0	0	0	0
NO_3	wall1	wall1-NO_3			0.02 - 0.15	0	0	0	0	0
N_2O_5	wall2	wall2-N_2O_5			0.01 - 0.08	0	0	0	0	0

Table S3. Sensitivity analysis of the effect of varying k_{w_{LFR},NO_3} on NO_{3exp}. The following inputs to the KinSim mechanism were assumed: $[NO_2]_{0,LFR}$ = $[O_3]_{0,LFR}$ = 300 ppm, T_{LFR} = T_{OFR} = 24°C, RH_{LFR} = RH_{OFR} = 1%, k_{w_{LFR},N_2O_5} = 0.1 s^{-1}, k_{w_{OFR},N_2O_5} = 0.014 s^{-1}, τ_{LFR} = 20 s, τ_{OFR} = 120 s, dilution factor = 4.4 between LFR and OFR.

k_{w_{LFR},NO_3} [s^{-1}]	NO_{3exp} [molecules cm^{-3} s]	Normalized NO_{3exp}
0	1.277×10^{14}	1
0.1	1.275×10^{14}	0.9984
0.2	1.273×10^{14}	0.9969
0.3	1.272×10^{14}	0.9965

Table S4. KinSim mechanism used to model destruction of alkyl and acyl organic peroxy radicals formed from VOC + NO_3 reactions in the OFR. Kinetic data is adapted from (Orlando and Tyndall, 2012).

Reactant 1	Reactant 2	Product 1	Product 2	Product 3	A_∞	E_∞	n_∞	A_0	E_0	n_0
VOC	NO_3	alkylRO2			0 or 2.5E-12	0	0	0	0	0
VOC	NO_3	acylRO2			2.5E-12 or 0	0	0	0	0	0
alkylRO2	NO				2.7E-12	-360	0	0	0	0
acylRO2	NO				7.5E-12	-290	0	0	0	0
alkylRO2	NO2	alkylRO2NO2			6.1E-12	0	0	1.3E-30	6.2	0.31
alkylRO2NO2		alkylRO2	NO2		8.8E+15	10440	0	0.00048	9285	0.31
acylRO2	NO2	acylRO2NO2			1.2E-11	0	0.9	2.7E-28	7.1	0.3
acylRO2NO2		acylRO2	NO2		5.4E+16	13830	0	0.0049	12100	0.3
alkylRO2	NO3	alkylRO	NO2		2.4E-12	0	0	0	0	0
acylRO2	NO3	acylRO	NO2		3.2E-12	0	0	0	0	0
alkylRO2	HO2				7.4E-13	-700	0	0	0	0
acylRO2	HO2				5.2E-13	-980	0	0	0	0
alkylRO2	acylRO2				2.2E-12	-500	0	0	0	0
acylRO2	acylRO2				2.9E-12	-500	0	0	0	0

Table S5. Bimolecular rate coefficients between selected biogenic volatile organic compounds (BVOCs) and NO_3, and BVOC + NO_3 carbonyl oxidation produts and NO_3. Rate coefficients were otained from Ng et al. (2017) and references therein, and are given in units of cm^3 $molecule^{-1}$ s^{-1}.

BVOC	k_{NO_3}	Oxidation Product	k_{NO_3}
isoprene	6.5×10^{-13}	methyl vinyl ketone	$<6\times10^{-16}$
		methacrolein	3.4×10^{-15}
α-pinene	6.2×10^{-12}	pinonaldehyde	2.0×10^{-14}
3-carene	9.1×10^{-12}	caronaldehyde	2.5×10^{-14}
sabinene	1.0×10^{-11}	sabinaketone	3.6×10^{-16}

References

Atkinson, R.: Kinetics and Mechanisms of the Gas-Phase Reactions of the NO_3 Radical with Organic Compounds, Journal of Physical and Chemical Reference Data, 20, 459–507, https://doi.org/http://dx.doi.org/10.1063/1.555887, 1991.

Atkinson, R., Aschmann, S. M., and Carter, W. P. L.: Kinetics of the reactions of O3 and OH radicals with furan and thiophene at 298 ± 2 K, International Journal of Chemical Kinetics, 15, 51–61, https://doi.org/10.1002/kin.550150106, https://onlinelibrary.wiley.com/doi/abs/10.1002/kin.550150106, 1983.

Atkinson, R., Arey, J., Zielinska, B., and Aschmann, S. M.: Kinetics and nitro-products of the gas-phase OH and NO_3 radical-initiated reactions of naphthalene-d8, fluoranthene-d10, and pyrene, International Journal of Chemical Kinetics, 22, 999–1014, https://doi.org/10.1002/kin.550220910, 1990.

Atkinson, R., Arey, J., Tuazon, E. C., and Aschmann, S. M.: Gas-phase reactions of 1,4-benzodioxan, 2,3-dihydrobenzofuran, and 2,3-benzofuran with OH radicals and O3, International Journal of Chemical Kinetics, 24, 345–358, https://doi.org/10.1002/kin.550240404, https://onlinelibrary.wiley.com/doi/abs/10.1002/kin.550240404, 1992.

Bernard, F., Magneron, I., Eyglunent, G., Daële, V., Wallington, T. J., Hurley, M. D., and Mellouki, A.: Atmospheric Chemistry of Benzyl Alcohol: Kinetics and Mechanism of Reaction with OH Radicals, Environ. Sci. Technol., 47, 3182–3189, https://doi.org/10.1021/es304600z, https://doi.org/10.1021/es304600z, 2013.

Boyd, C. M., Sanchez, J., Xu, L., Eugene, A. J., Nah, T., Tuet, W. Y., Guzman, M. I., and Ng, N. L.: Secondary organic aerosol formation from the β-pinene+NO_3 system: effect of humidity and peroxy radical fate, Atmospheric Chemistry and Physics, 15, 7497–7522, 2015.

Cantrell, C. A., Davidson, J. A., Shetter, R. E., Anderson, B. A., and Calvert, J. G.: Reactions of nitrate radical and nitrogen oxide (N2O5) with molecular species of possible atmospheric interest, The Journal of Physical Chemistry, 91, 6017–6021, https://doi.org/10.1021/j100307a040, https://doi.org/10.1021/j100307a040, 1987.

Chew, A. A., Atkinson, R., and Aschmann, S. M.: Kinetics of the gas-phase reactions of NO3 radicals with a series of alcohols, glycol ethers, ethers and chloroalkenes, J. Chem. Soc., Faraday Trans., 94, 1083–1089, https://doi.org/10.1039/A708183I, http://dx.doi.org/10.1039/A708183I, 1998.

D'Anna, B., Andresen, Ø., Gefen, Z., and Nielsen, C. J.: Kinetic study of OH and NO_3 radical reactions with 14 aliphatic aldehydes, Phys. Chem. Chem. Phys., 3, 3057–3063, https://doi.org/10.1039/B103623H, 2001.

Ng, N. L., Brown, S. S., Archibald, A. T., Atlas, E., Cohen, R. C., Crowley, J. N., Day, D. A., Donahue, N. M., Fry, J. L., Fuchs, H., Griffin, R. J., Guzman, M. I., Herrmann, H., Hodzic, A., Iinuma, Y., Jimenez, J. L., Kiendler-Scharr, A., Lee, B. H., Luecken, D. J., Mao, J., McLaren, R., Mutzel, A., Osthoff, H. D., Ouyang, B., Picquet-Varrault, B., Platt, U., Pye, H. O. T., Rudich, Y., Schwantes, R. H., Shiraiwa, M., Stutz, J., Thornton, J. A., Tilgner, A., Williams, B. J., and Zaveri, R. A.: Nitrate radicals and biogenic volatile organic compounds: oxidation, mechanisms, and organic aerosol, Atmospheric Chemistry and Physics, 17, 2103–2162, https://doi.org/10.5194/acp-17-2103-2017, 2017.

Orlando, J. J. and Tyndall, G. S.: Laboratory studies of organic peroxy radical chemistry: an overview with emphasis on recent issues of atmospheric significance, Chem. Soc. Rev., 41, 6294–6317, https://doi.org/10.1039/C2CS35166H, 2012.

Palm, B. B., Campuzano-Jost, P., Day, D. A., Ortega, A. M., Fry, J. L., Brown, S. S., Zarzana, K. J., Dube, W., Wagner, N. L., Draper, D. C., Kaser, L., Jud, W., Karl, T., Hansel, A., Gutiérrez-Montes, C., and Jimenez, J. L.: Secondary organic aerosol formation from in situ OH, O_3, and NO_3 oxidation of ambient forest air in an oxidation flow reactor, Atmospheric Chemistry and Physics, 17, 5331–5354, https://doi.org/10.5194/acp-17-5331-2017, 2017.

Toby, S., Van de Burgt, L. J., and Toby, F. S.: Kinetics and chemiluminescence of ozone-aromatic reactions in the gas phase, J. Phys. Chem., 89, 1982–1986, https://doi.org/10.1021/j100256a034, https://doi.org/10.1021/j100256a034, 1985.